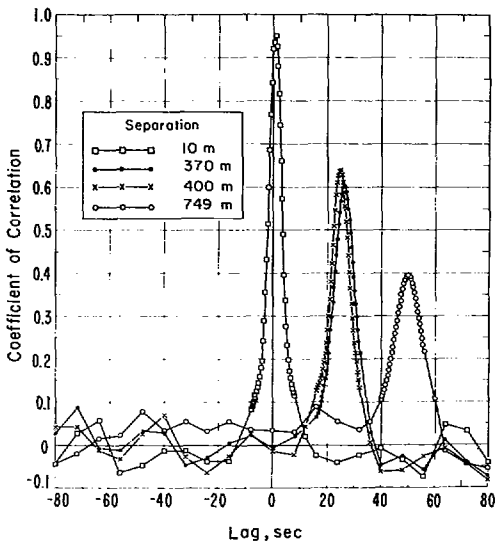

Fig. 13. Cross-correlation functions of same data used in Fig. 12, after taking first differences to remove trends and to sharpen maxima.

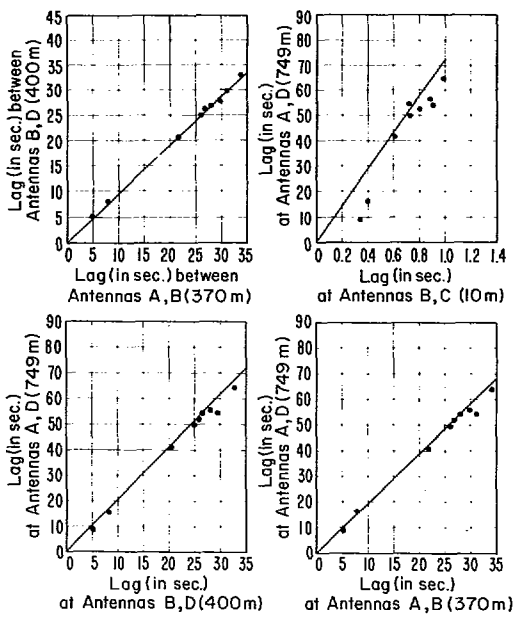

Fig. 14. Comparison of time lags at different path separations.

the data are dominated by slowly varying trends (as was also shown by the steep power spectra discussed previously). The correlation of first differences of values spaced arbitrarily 4-s apart was also computed to remove the effect of trends and sharpen the maxima, and the corresponding results are shown in Fig. 13.

The lags for maximum correlation observed on any two pairs of paths proved to be closely correlated from sample to sample and the amount of lag was very nearly proportional to path separation. This is illustrated in Fig. 14, in which the lag values are cross-plotted for each of the four combinations of path separation. The line drawn across each graph represents the theoretical locus of lags proportional to path separation.

IV. Summary

The experiment reported here has yielded a statistical description of tropospheric noise to be expected in azimuth angle measurements made at low elevation angles with a baseline range-differencing microwave system. The results show a monotonic decrease in rms angular noise as the baseline length is increased from 10 to 749 m. However, the relationship between rms angular noise and baseline length is strongly influenced by the length of the period of measurement, and this is explained by reference to the power spectra of the range and range-difference data. These spectra indicate that for all but the shortest baseline, the data are dominated by large, slow variations.

A cross-correlation analysis of range variations occurring at the four baseline antennas indicated that the spatial refractive index structure of the atmosphere remained essentially "frozen" as it was carried across the four propagation paths by the prevailing wind.

References

[1] H. B. Janes and M. C. Thompson, Jr., "Errors induced by the atmosphere in microwave range measurements," *Radio Sci.*, vol. 68D, no. 11, pp. 1229–1235, Nov. 1964.
[2] K. A. Norton, J. W. Herbstreit, H. B. Janes, K. O. Hornberg, C. F. Peterson, A. F. Barghausen, W. E. Johnson, P. I. Wells, M. C. Thompson, Jr., M. J. Vetter, and A. W. Kirkpatrick, "An experimental study of phase variations in line-of-sight microwave transmissions," Nat. Bur. Stand., Boulder, Colo., NBS Monogr. 33, Nov. 1961.
[3] M. C. Thompson, Jr., "The effects of propagation on measurements of distance, angle-of-arrival, and Doppler effect in ground-to-ground systems," in *1966 Proc. URSI Gen. Assembly, Progr. in Radio Sci., 1963–1966*, Part I, pp. 579–595.
[4] H. B. Janes, "Atmospheric errors in electromagnetic distance measurements, ESSA-Hawaii experiments, 1966–67," in *1967 Proc. AGARD-EPC 13th Symp.*
[5] H. B. Janes, M. C. Thompson, Jr., D. Smith, and A. W. Kirkpatrick, "Comparison of simultaneous line-of-sight signals at 9.6 and 34.5 GHz," *IEEE Trans. Antennas Propagat.*, vol. AP-18, pp. 447–451, July 1970.
[6] M. C. Thompson, Jr., and H. B. Janes, "Effects of sea reflections on phase of arrival of line-of-sight signals," *IEEE Trans. Antennas Propagat.*, vol. AP-19, pp. 105–108, Jan. 1971.
[7] M. C. Thompson, Jr., and M. J. Vetter, "Single path phase measuring system for three-centimeter radio waves," *Rev. Sci. Instrum.* vol. 29, no. 2, pp. 148–150, Feb. 1958.
[8] G. M. Jenkins and D. G. Watts, *Spectral Analysis and Its Applications*. San Francisco, Calif.: Holden-Day, 1968.
[9] V. I. Tatarski, *Wave Propagation in a Turbulent Medium*. New York: Dover, 1967.
[10] D. K. Barton, *Radar System Analysis*. Englewood Cliffs, N. J.: Prentice-Hall, 1964.
[11] F. Pasquill, *Atmospheric Diffusion*, New York: VanNostrand Rheinhold, 1961.
[12] R. W. Lee and A. T. Waterman, Jr., "Space correlations of 35-GHz transmissions over a 28-km path," *Radio Sci.*, vol. 3, pp. 135–139, Feb. 1968.

A New Inversion Method in Electromagnetic Wave Propagation

P. EDENHOFER, J. N. FRANKLIN, AND C. H. PAPAS

***Abstract*—A theoretical investigation by an integral equation approach for the determination of the atmospheric refractive index profile from satellite radio tracking data is reported. A numerical solution is constructed by applying a minimum mean-squared estimator. An iterative procedure is suggested and shown to be convergent.**

I. Introduction

A nonlinear integral equation of the first kind and of Fredholm type relates the atmospheric refractive index as a function of space to the radio tracking data from a satellite as a function of the satellite's elevation angle. The radio tracking data are affected by EM wave propagation phenomena which in the VHF range (e.g., 136 MHz) are mainly due to the ionosphere. Such an integral

Manuscript received July 14, 1971; revised November 7, 1972. This work was supported by the Deutsche Forschungs- und Versuchsanstalt für Luft- und Raumfahrt (DFVLR), the German Federal Ministry for Education and Science, and NASA under International University Fellowship.

P. Edenhofer was a Research Fellow at the Department of Electrical Engineering, California Institute of Technology, Pasadena, Calif. He is now with DFVLR-Institut für Flugfunk und Mikrowellen, 8031 Oberpfaffenhofen, Germany.

J. N. Franklin and C. H. Papas are with the Division of Engineering and Applied Science, California Institute of Technology, Pasadena, Calif. 91103.

equation must be solved, if one is interested in determining from an analysis of the radio tracking data not only the ionospheric electron content (integrated profile) but also the profile itself, i.e., the spatial distribution of the electrons in the ionosphere. Making use of a model-fitting approach gives only the gross structure of the profile [1]. It is the inversion method approach that provides information on this and on the fine structure of the refractive index profile as well. Work has already been done in this field by using an integral equation approach, such as the well-known derivation of the lower electron density profile by a ground-based probing of the ionosphere [2]; the passive probing of the troposphere using the microwave spectrum of oxygen [3]; and the inversion of occultation data from spacecrafts to explore planetary atmospheres [4], [5].

II. Linearized Integral Equation

We consider the case of range tracking data (range errors due to EM wave propagation at VHF) as a specific example, and assume that the ionosphere as the dominant refractive medium is stationary, isotropic, and spherically stratified. Thus the refractive index profile associated with the medium is understood to be an "equivalent vertical profile."

Making use of the principles of geometrical optics one can show that the following relationship holds [1], [6]:

$$e(s) = \int_a^b K[n(r); s,r]\, dr. \tag{1}$$

The quantity e denotes the range error as a function of the antenna's elevation angle θ which varies during a satellite's passage ($s = \cos\theta, 0 < \theta < 90°$). The lower and upper boundaries of the refractive medium are given by a and b, respectively; r denotes the radial coordinate in a geocentric reference system ($a \leq r \leq b$). The left-hand side of (1) is the difference between the range data actually measured and the range data resulting from the ray geometry outside the refractive medium as computed by an orbit determination program based on celestial mechanics ($e = u - v$).

In a dispersive medium the integral kernel $K = K_g$ involves the group path and is given by

$$K = \frac{1}{n}\left(1 - \frac{\alpha^2}{n^2}\right)^{-1/2} = (n^2 - \alpha^2)^{-1/2} \tag{2}$$

where $\alpha(s,r) = n'r'(s/r) < 1$ with r' as the mean radius of the earth ($n' = 1$). In case of phase path (involving Doppler tracking data), $K = K_p$ can be derived from $K_p = n^2 K_g$ (Papas [7]). The function $\alpha(s,r)$ is introduced through Snell's law. The nonlinearity of the kernel K with respect to the unknown profile $n(r)$ is due to the time delay (proportional to $1/n$) and the refraction suffered by the EM wave in the ionospheric medium. All functions appearing in (1) are real functions. The limits of integration are finite and the value of the kernel remains finite within the integration interval, i.e., the integral equation is nonsingular.

Equation (1) is linearized by setting

$$n(r) = n^{(0)}(r) + n^{(1)}(r) \tag{3}$$

where $n^{(0)}$ represents a reference profile (e.g., Chapman model profile). The term $n^{(1)}$ represents the perturbation profile to be solved for. From a Taylor series expansion of K around $n^{(0)}$, it follows

$$K(n) = K(n^{(0)} + n^{(1)}) = K^{(0)} + K^{(1)}n^{(1)} + 0[(n^{(1)})^2]. \tag{4}$$

Introducing (4) into (1) the following linearized integral equation is obtained:

$$e^{(1)}(s) = \int_a^b K^{(1)}(s,r)n^{(1)}(r)\, dr \tag{5}$$

where

$$e^{(1)}(s) = u(s) - v(s) - e^{(0)}(s)$$

$$e^{(0)}(s) = \int_a^b K^{(0)}(s,r)\, dr.$$

Here $e^{(0)}(s)$ is the range error when the perturbation profile is zero; $K^{(0)}$ and $K^{(1)}$ are known in terms of $n^{(0)}$ and α.

Generally integral equations like (5) are ill posed, i.e., small variations in $e^{(1)}$ might give rise to large variations in $n^{(1)}$. According to Franklin [8] a well-posed stochastic extension can be obtained from (5) by interpreting $e^{(1)}$ and $n^{(1)}$ realistically as random variables and by taking into account an additional term, which incorporates the range errors inevitably introduced by the computational procedure (digital representation, roundoff, etc.) and, more importantly, by the technique of measurement (ground reflections, receiver noise, etc.). By reducing (5) to a matrix equation, one thus gets

$$A^{(1)}n^{(1)} + f = e^{(1)} \tag{6}$$

with $A^{(1)} = A^{(1)}(s_i,r_j) = K^{(1)}(s_i,r_j)w_j\Delta r_j$ evaluated at m different angles $s_i = \cos\theta_i$, $i = 1,2,\cdots,m$, and involving n quadrature abscissas of the perturbation profile $n^{(1)} = n^{(1)}(r_j)$ with weights w_j, $j = 1,2,\cdots,n$.

III. Optimization

A numerical solution to (6) is constructed by minimizing the following mean-squared expectation [8]

$$E[X^*X] = \min$$

$$X = n^{(1)*}a_1 - e^{(1)*}a_2. \tag{7}$$

The superscript asterisk indicates adjoint quantities. The success of estimation is measured with respect to an arbitrary, nonzero vector a_1 in Hilbert space H_n defined by the random process with samples $n^{(1)}$. A bounded, linear transformation is expected to hold between a_1 and a_2 (i.e., optimal estimation by orthogonal projection of random vectors on an appropriate linear space). The profile $n^{(1)} = \hat{n}^{(1)}$, optimal with respect to criterion (7), turns out to be

$$\hat{n}^{(1)} = C_{nn}A^{(1)*}(A^{(1)}C_{nn}A^{(1)*} + C_{ff})^{-1}e^{(1)} \tag{8}$$

under the assumption that there is no bias. Here C_{nn} and C_{ff} denote the covariance matrices for the sample vectors $n^{(1)}$ and f, respectively, which are supposed to be stationary and statistically independent ($C_{nf} = C_{fn} = 0$). In case of perfect range measurements ($C_{ff} = 0$), (8) reduces to $\hat{n}^{(1)} = (A^{(1)})^{-1}e^{(1)}$, which is the classical nonoptimal solution of the corresponding ill-posed matrix equation ($m = n$).

The following statistical model is suggested in the construction of the covariance matrices involved:

$$C_{nn} = E[n_i^{(1)}n_j^{(1)*}] = \frac{\gamma}{\rho(2\pi)^{1/2}} \exp\left[-\frac{(r_i - r_j)^2}{2\rho^2}\right]$$

$$C_{ff} = E[f_i f_j^*] = \nu_i^2\delta_{ij} \tag{9}$$

with $i,j = (1,2,\cdots,n \text{ or } m)$ for C_{nn} and C_{ff}, respectively.

It seems reasonable to assume that the statistical variations of the refractive index are correlated in terms of a Gaussian distribution ("size" γ and "smoothness" ρ known from ionospheric observations) and that f has the character of white noise (measurements at different elevation angles being independent of each other). The standard deviations ν_i (known, at least to some extent, from estimation) are expected to be maximum at low elevation angles and to decrease towards the culmination point of the satellite's passage. The reliability of estimation associated with (8) and further details will be discussed elsewhere.

IV. Iterative Procedure

Now, as a generalization of (3), the solution obtained so far will be improved by an iterative procedure. Specifically, we take

$$n^{(k+1)} = n^{(k)} + N^{(k+1)}, \qquad k = 0,1,\cdots,p-1. \tag{10}$$

At each step of the iteration (p at maximum), the calculations according to (5), (8), and (10), done by a profile correction program (PCP), are to be combined with those resulting from an orbit determining program (ODP). Thus the v values from (5) can be corrected for the PCP's refractive index profile $n^{(k)}$, which affects the satellite's orbit determination in analysis of the radio tracking data ($v = v^{(k)}$).

It can be shown that the following recurrence relation holds in proving the convergence of the iterative procedure (10):

$$\epsilon^{(k)} - \epsilon^{(k+1)} = N^{(k+1)} = A_k\epsilon^{(k)} + B_k\epsilon^{(k)2} \tag{11}$$

where

$$\epsilon^{(k)}(r) = n(r) - n^{(k)}(r), \qquad A_k, B_k \neq 0.$$

The quantities $\epsilon^{(k)}$ and $\epsilon^{(k+1)}$ denote the deviation of the approximate, iterated perturbation profile for $r = r_j$ at the kth and $(k+1)$th step of iteration, respectively, from the exact but unknown profile solving (1). The iterative procedure turns out to be of first order ($A_k \neq 0$).

To start the iterative procedure successfully (i.e., $|\epsilon^{(1)}| < |\epsilon^{(0)}|$), (11) requires that an inequality relation be satisfied by the initial ($k = 0$) deviation

$$\frac{1}{b_0}\frac{1-a_0}{1+a_0} < \epsilon^{(0)} = n - n^{(0)} < -\frac{1}{b_0} \tag{12}$$

where

$$a_0 = \left.\frac{\partial V}{\partial g}\right|_{g=g(0)} = \frac{\partial V}{\partial g}$$

$$b_0 = \frac{1}{2}\frac{\partial^2 K/\partial n^{(0)2}}{\partial K/\partial n^{(0)}} = -\frac{2n^{(0)2}+\alpha^2}{2n^{(0)}(n^{(0)2}-\alpha^2)} < 0, \qquad K = K_\varrho.$$

The parameter a_0 is defined by assuming a very general functional relationship for the coupling term $v^{(k)}(s) = V(s,g^{(k)}(s))$ with $g(s) \triangleq e(s)$, likewise (1). Relation (12) can actually be satisfied by the parameter combination: $a_0 > 0$, $b_0 < 0$. Condition $a_0 > 0$ means in practice that the uncertainty of determining the satellite's position in space grows with increasing values for the residual propagation errors g inherent to the ODP. Obviously this has to be expected for any tracking situation. The condition $b_0 < 0$ is always satisfied as far as the wave's group path is concerned. In case of phase path, b_0 is only negative for elevation angles greater than some 45°.

Now the plausible result from (12) is that $|\epsilon^{(0)}|_{\max}$ is proportional to a quantity describing how sensitive the kernel $K(n)$ is as to variations of the refractive index. On the other hand, $|\epsilon^{(0)}|_{\max}$ decreases with increasing inability of the ODP to locate the satellite's position ($|\epsilon^{(0)}|_{\max} \to 0$, $a_0 \to \infty$). Thus the maximum admissible initial deviation is given by

$$|\epsilon^{(0)}|_{\max} = 2\frac{1}{|b_0|}\frac{1}{1+a_0} \leq 2\frac{1}{|b_0|}. \tag{13}$$

After a certain number of iterative steps the procedure (10) can be expected to be of second order with $a_k \to 0$, $A_k \to 1$ (weak coupling between PCP and ODP)

$$|\epsilon^{(k+1)}| = |B_k|\,\epsilon^{(k)2} \tag{14}$$

relating the deviations of two successive steps to each other as in (11). Once this step of iteration is attained the sequence of ϵ values converges rather slowly at first, but then convergence is extremely fast depending on how much smaller $|B\epsilon|$ is than one.

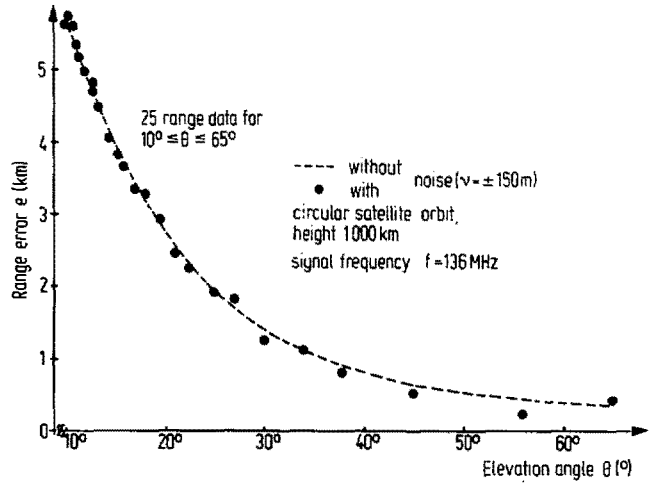

Fig. 1. Simulated VHF-range data corrupted by Gaussian noise.

At high elevation angles ($\theta > \theta_{\max}$; e.g., $\theta_{\max} = 85°$) any integral kernel $K^{(k)}(s,r)$ depends only slightly on the radial coordinate r according to (2), (4). In this case the integral equations (1) and (5) are degenerate, yielding for example

$$e^{(1)}(s) \approx \overline{K^{(1)}(s)} \int_a^b n^{(1)}(r)\,dr. \tag{15}$$

From (15) it is clear that only integrated values of the refractive index profile can be determined (e.g., electron content), but not the profile itself. When solving for the profile by using (8) and (10), all range data belonging to $\theta > \theta_{\max}$ must be excluded, since such data would cause the elements of the corresponding rows of the matrix to become equal (det $A = 0$).

V. Numerical Results

In order to demonstrate the principal feasibility and the practical usefulness of the inversion method, the theoretical calculations outlined were proved by test computations. Since actual range tracking data were not available, these computations were performed by using simulated, pseudorange tracking data from a satellite supposed to have a circular orbit at a height of 1000 km and a signal frequency of 136 MHz.

Fig. 1 shows the range error versus the topocentric elevation angle. The dashed curve represents the values assuming an ionospheric test profile of Chapman type with parameters $f_N = 10$ MHz; $h_m = 330$ km; $H = 60$ km. As indicated, 25 discrete range data were corrupted by Gaussian noise with a standard deviation $\nu = \pm 150$ m.

These data were taken to reconstruct the test profile via (8) by starting from a reference profile $n^{(0)}$ with Chapman parameters different from those of the test profile. The numerical results for some values of the refractive index along the profile are given in Fig. 2 (16-point Gaussian quadrature; C_{nn}: $\gamma = 10^{-7}$, $\rho = 5$ km). The results show that around the height of maximum ionization (down to some 250 km and up to some 400 km) the values of the perturbation profile are in good agreement with those of the test profile depending on the number of iterative steps; e.g., for $k = 5$ the remaining errors are in the order of about 10 to 20 percent. At the lower and upper boundary of the ionosphere the reconstruction of the test profile turns out to be less successful. The remaining errors increase up to 50 or 60 percent. The condition number associated with such a typical example of data analysis amounts to about 2×10^5. The condition number of the corresponding ill-posed, highly unstable problem increases (order of magnitude 10^{13}), causing the numerical results to be divergent.

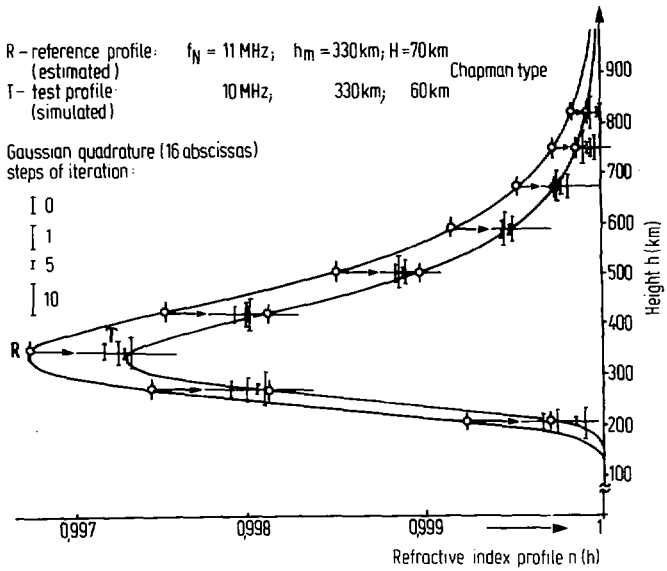

Fig. 2. Reconstruction of test profile for refractive index depending on number of iterative steps.

At present two concluding remarks are to be added: Firstly, the choice of a specific numerical integration procedure and the number of quadrature abscissas turn out to be critical. The Gaussian quadrature seems to be most promising, though its nodes are not properly located along the profile. Secondly, the modeling of the covariance matrices turns out to be critical, too. The statistical model used and its parameters involved strongly influence the success of estimation.

VI. Conclusions

Obviously the inversion method presented here to determine the electron density in the ionosphere may also be applicable numerically to solve other ill-posed, nonlinear problems which can be formulated as integral equations. The very general and fundamental background of such problems in electromagnetic wave propagation is to find the spatial distribution of dielectric matter in inhomogeneous media from an analysis of specific propagation phenomena, e.g., depending on the angle of incidence or the frequency of a wave.

Acknowledgment

Gratitude is expressed to Dr. A. J. Kliore, Dr. W. G. Melbourne (JPL), and Prof. D. O. Muhleman (Caltech) for their valuable discussions. Gratitude is also expressed to Dr. E. Lüneburg and Dr. V. Stein (DFVLR) for their cooperation in performing the numerical computations of Section V.

References

[1] P. Edenhofer, "Variations of tropospheric and ionospheric models and parameters affecting the propagation of satellite signals," in *Proc. 17th Int. Astronaut. Congr.*, vol. II, pp. 105–116, Oct. 1966.
[2] K. G. Budden, *Radio Waves in the Ionosphere*. Cambridge, England: Cambridge University Press, 1961.
[3] E. R. Westwater and O. N. Strand, "Statistical information content of radiation measurements used in indirect sensing," *J. Atmos. Sci.*, vol. 25, pp. 750–758, Sept. 1968;
[4] A. Kliore *et al.*, "Occultation experiment: results of the first direct measurement of Mars' atmosphere and ionosphere," *Science*, vol. 149, pp. 1243–1248, 1965.
[5] G. Fjeldbo and V. R. Eshleman, "The atmosphere of Mars analyzed by integral inversion of the Mariner IV occultation data," *Planet. Space Sci.*, vol. 16, pp. 1035–1059, 1968.
[6] A. Sommerfeld, "Theoretische Physik," Germany: Geest und Portig, 1959, Bd. IV.
[7] C. H. Papas, *Theory of Electromagnetic Wave Propagation*. New York: McGraw-Hill, 1965.
[8] J. N. Franklin, "Well-posed stochastic extensions of ill-posed linear problems," *J. Math. Anal. Appl.*, vol. 31, pp. 682–716, 1970.
[9] J. Anderson, D. O. Muhleman *et al.*, "Determination of astrodynamic constants and a test of the general relativistic time delay with *S*-band range and Doppler data from Mariners 6 and 7", presented at 13th Cospar Meeting, Leningrad, U.S.S.R., May 1970.

Comparison of Observed and Predicted Phase-Front Distortion in Line-of-Sight Microwave Signals

HARRIS B. JANES AND MOODY C. THOMPSON, JR.

***Abstract*—Two experiments are reported which were designed to demonstrate the theoretical relationship between the phase-front distortion of line-of-sight microwave signals and the refractive index structure along the propagation path. Measurements were made on a slanted 64-km path in Hawaii with an elevation angle of 2.5°, using a horizontal array of 4 antennas at the upper terminal to observe the phase structure function, and an airborne refractometer to measure the refractive index structure. The predicted phase structure function computed from the refractometer data is compared with the observed structure function, and shows best agreement in the periods 0100–0700 hour and 1300–1900 hour.**

I. Introduction

Porcello has applied Tatarski's basic theory of wave propagation through a turbulent medium to the prediction of phase errors across the synthetic aperture of a side-looking terrain-imaging radar [1], [2]. The prediction depends on knowledge of the refractive index structure parameter C_n along the propagation path.

To investigate this proposed method, two experiments were conducted in 1968 in which phase-front variations at the upper terminal of a fixed slanted propagation path and refractive index variations in the neighborhood of the path, were measured simultaneously. This report gives a comparison of the observed phase-front structure function with the corresponding values computed from the refractive index data. The radio measurements in this experiment were similar to those made in 1964 on an overland path [3]. In the earlier work, atmospheric data were available only at the path terminals. In the present experiment, a longer overwater path was used, and concurrent refractive index measurements were taken along the propagation path to provide the basis for an evaluation of the prediction method.

II. Description of Experiments

The experiments were conducted during two 2-week periods in April and November 1968 using a slanted, 64-km propagation path in Hawaii, A map and vertical profile of the path are shown in [8, figs. 1 and 2]. A sketch of the experimental arrangement is shown in Fig. 1.

The refractive index data were obtained with a solid-state microwave refractometer [4] in a light aircraft. The flight schedule called for two flights per day, spaced about 6 h apart, with the starting time advanced 3 h each day. In principle, data could thus be obtained from about 24 flights covering essentially all times of the day in the course of each of the 2-week experiments. Many of the scheduled flights were omitted because of rain and/or heavy cloudiness and the restriction to visual flight rules. As a result, and because of occasional equipment difficulties, simultaneous phase and refractive index data were obtained from 13 flight periods in April, and from 18 in November.

Each flight consisted of an ascent (at approximately midpath) to an altitude of 3 km, and a descent in a "ladder" pattern with 10 level flight segments about 2.5-km long, perpendicular to the propagation path, and with a vertical separation of 300 m. Each descent required a period of about 45 min to 1 h.

During each flight, an analog magnetic tape recording was made of refractive index variations during both the ascent and descent.

Manuscript received September 21, 1972; revised September 25, 1972. This work was supported by the U. S. Air Force Avionics Laboratory under Delivery Order AF 33(615)66-5002.
The authors are with the Office of Telecommunications, Institute for Telecommunication Science, U. S. Department of Commerce, Boulder, Colo. 80302.